AIAA

# COLLINEAR THREE-CRAFT COULOMB FORMATION STABILITY ANALYSIS AND CONTROL

Drew R. Jones and Hanspeter Schaub

AIAA/AAS Astrodynamics Specialist Conference, Minneapolis, MN, August 13–16, 2012

# Collinear Three-Craft Coulomb Formation Stability Analysis and Control

Drew R. Jones*

*The University of Texas at Austin, Austin, TX, 78712*

and Hanspeter Schaub†

*University of Colorado, Boulder, CO, 80309*

**Controlling the Coulomb forces of charged close-flying craft is a highly efficient way to enable static formation equilibria, in which craft separation distances remain constant. But maintaining and maneuvering these inherently unstable formations, particularly with limited Coulomb force controllability, is challenging. This paper studies 3-craft collinear equilibria, admitted in the presence of a central-body gravity field. Previous research establish necessary conditions for 3-craft collinear Coulomb formations, and this paper develops necessary and sufficient conditions, considering a more accurate Coulomb force model. Stability properties for each of the resulting configurations are analyzed for the first time. Specifically, it is shown that each equilibrium can be designed to have marginal stability normal to the orbit-plane. Also, it is demonstrated that for the radially aligned configuration, in-plane perturbations can be asymptotically stabilized, using only Coulomb forces. A charge feedback law is derived, and numerical results are provided. Similar stability properties are known and utilized for 2-craft formations, but were previously unknown for these 3-craft equilibria. Finally, invariant manifolds are generated to illustrate some dynamical properties of this class of Coulomb formation, also for the first time. The possibility of exploiting the manifold flows to target, minimum inertial thrust, reconfigurations which realize the useful shape-changing ability of these systems, is discussed.**

## I. Introduction

Spacecraft charge control was considered as early as 1966 by Cover, Knauer, and Maurer,[1] who proposed to use electrostatic forces to inflate and maintain the shape of a large reflecting mesh. The prospect of using this concept in spacecraft formation flying is introduced by King et al.,[2,3] where the electric potential (or net charge) of each vehicle is actively controlled, to yield desired inter-craft forces. Close-proximity spacecraft have many advantages over a single large craft, including: overall mass reduction, shape-changing ability, and multiple launches for deployment, assembly, and repair. Free-flying formations have applications in Earth imaging, surveillance, and for enabling separated space-borne interferometry.[2,4] Initially, electric propulsion (EP) systems were proposed for controlling the relative craft motions; however, EP suffers from limited throttle-ability and introduces the problem of thruster-plume impingement, where thruster ejecta may damage or impede neighboring craft.[2] In contrast, active charge control avoids thruster-plumes, has fast throttling (ms transitions), and can sustain a given force using less power and fuel than EP.[1,2] Charge control is highly efficient with *ISP*$\sim 10^{13}$ s, and is based on existing technology. Active control of spacecraft charge was successfully executed during the SCATHA[5] and ATS[6] missions, and currently on the CLUSTER[7] mission. other applications for electrostatic thrusting include: advanced docking/rendezvous, autonomous inspection, contact-less removal of hazardous material, and the deployment/retrieval of instruments.[8]

Of particular interest in Coulomb formation flying are constant charge 'virtual structures', referred to as static Coulomb formations, in which craft separation distances are in equilibrium. Charge control is

*Graduate Student, Aerospace Engineering and Engineering Mechanics Department, WRW Laboratories, The University of Texas at Austin. drjones604@utexas.edu

†Associate Professor, H. Joseph Smead Fellow, Department of Aerospace Engineering Sciences, University of Colorado.

demonstrated to be a capable and efficient means for establishing and maintaining geometries which appear frozen, with respect to the Hill-frame, a rotating frame with origin at the formation center-of-mass.[2,8] Milli-Newton levels of forces can be produced over dozens of meters using only Watt-levels of electrical power. Necessary equilibrium conditions are derived for such formations, analytically for less than 5 craft (numerically otherwise), and thus far, all are dynamically unstable.[2,8] It is the 3-craft collinear, Hill-Frame equilibria, in the presence of linearized gravity, which are considered in the current work. This research expands upon the work of Berryman and Schaub,[8] by deriving sufficient equilibria conditions and by including the physical effect of plasma shielding. These sufficient conditions yield unique equilibrium regions with varying stability properties, which are explored in detail for the first time. Analogous explicit existence criteria are defined for spinning 3-craft collinear equilibria, in the absence of gravitational forces,[9,10] and Wang and Schaub expand these to be sufficient for real-valued charges.[11] Stability analyses are carried out for 2- and 3-craft spinning configurations,[12,13] and stable 2-body scenarios are identified when the plasma shielding is included.[12] A recent study by Hogan and Schaub demonstrate marginal in-plane stability of particular collinear spinning equilibria, if proper separation distance and speed conditions are met.[13]

Unfortunately, Coulomb thrusting has limited extent (from plasma shielding) and controllability, and for example cannot alter the overall formation angular momentum.[14] Therefore, it is often supplemented with the less desirable inertial thrust (e.g. EP or chemical), which necessitates hybrid control.[15,16] Methods for maintaining and maneuvering the inherently unstable Coulomb formations remains a challenging and active area of research. Natarajan and Schaub demonstrate that the Radial 2-craft Hill-frame equilibria has marginal out-of-plane stability and that charge control alone can asymptotically stabilize in-plane perturbations. In the current research, it is shown that the Radial 3-craft formation shares these properties, and an in-plane charge feedback law is derived to maintain the formation, substantiated by numerical simulation. Also, relative instability and eigenvector mode properties associated with all of the 3-craft collinear configurations are analyzed. In particular, marginal stabilities along particular Hill-axes are indicated in the interest of utilizing these facets to reduce station-keeping control effort. Marginal axis stability is exploited during controller design for the 2-craft Orbit-Normal configuration[15] and 3-craft spinning equilibria.[9,11,17,18] In addition, feedback control is derived by Inampudi for CRTBP equilibrium configurations about Earth-Moon libration points.,[16] and nonlinear controllers are considered and tested for 3-craft spinning equilibria.[9,17,18]

Another advantageous property of free-flying formations, is that they can change shape and therefore be reconfigured as necessary for a particular mission. Methods for realizing the shape-changing ability of Coulomb formations are just being explored, and doing so optimally is very new. Natarajan[19] presents a hybrid (Coulomb and inertial) feedback control to transfer between 2-craft Hill-frame configurations, and Inampudi adds optimization to those transfers by minimizing: time, fuel, or total power usage.[16] Jones and Schaub outline a generalized procedure for targeting minimal $\Delta V$ transfers between Coulomb equilibria, in which a parameter optimization formulation is used to differentially correct an uncontrolled, and discontinuous, initial trajectory along invariant manifolds.[20,21] This method seeks natural flows along manifolds that nearly 'hop' from unstable to stable branches, in order to partially achieve the reconfigurations, and thereby reduce $\Delta V$. This is analogous to work in which manifolds are used to design low-thrust transfers, in multi-body gravity fields, for example in the work of Russell and Lam.[22] In this paper, invariant manifold theory is applied to the 3-craft collinear equilibria, for the first time. The intention is to understand how the method of Jones and Schaub[20,21] may be utilized and extended, to achieve minimal $\Delta V$ shape-changes for this class of 3-craft Coulomb formation.

# II. Background and General Model

## A. Spacecraft Charge Control Background

A conductive craft surface will naturally exchange ions and electrons with the plasma of space, and as a result will assume a non-zero electric potential $\phi$ (measured in Volts). When immersed in a plasma, the ideal vacuum potential is effectively limited (or shielded) due to interactions with free particles and photons. The Debye length $\lambda_d$ approximates this shielding, such that a charged particle at a distance $r > \lambda_d$ is unaffected by $\phi$. Debye length is a measure of the time-dependent local plasma temperature and density, and experimental values for it have been acquired in various regimes (e.g. LEO: $0.02-0.4$ m, GEO: $140-1500$ m, Interplanetary: $7.4-24$ m).[2]

A steady-state $\phi$ occurs when the net current to the craft surface is zero,[2] and altering $\phi$ artificially has substantial mission heritage.[5–7] This involves utilizing an electron-gun or similar device to eject electrons/ions into the surrounding plasma with sufficient kinetic energy to escape the 'potential-well'. Therefore, the device must have sufficient power to supply a voltage equal to the desired $\phi$, at a current at least greater than the incoming environmental current (since this will tend to drive $\phi$ back to natural equilibrium). In this work, perfectly spherical spacecraft (radius $R_{sc}$) are assumed, and formations near GEO are considered. Each craft's net surface charge $q$ is considered as a control, by allowing $q$ to be analytically related to the truly measurable/controllable parameter $\phi$, via Eq. (1), where $k_c$ is the Coulomb constant.

$$\phi = k_c \frac{q}{R_{sc}} \tag{1}$$

Equation (1) holds in a vacuum so long as all spacecraft are assumed to have perfectly conductive outer surfaces, of uniform charge density. Additionally, it is accurate in the plasma so long as $R_{sc} \ll \lambda_d$ , and if the capacitance of a single is not impacted by neighboring charged craft. The former is true in the presumed GEO altitude, and the latter is a good assumption so long as the craft are sufficiently far apart, which will be enforced throughout this work.

## B. Dynamical Model

Formation dynamics are modeled relative to the Hill-frame, which is centered at and rotates with a nominal center-of-mass (CM) orbit (assumed circular with semi-major-axis $a_0$ near GEO), as shown in Figure 1. The Hill-frame axes are labeled: $\hat{e}_R$ for radial, $\hat{e}_T$ for transverse, and $\hat{e}_N$ for normal. The vehicles then appear statically fixed with respect to the rotating Hill-frame, for equilibrium configurations admitted by this model. The Hill-Frame introduces a CM constraint given by Eq. (2a), where craft $i$ of mass $m_i$ and

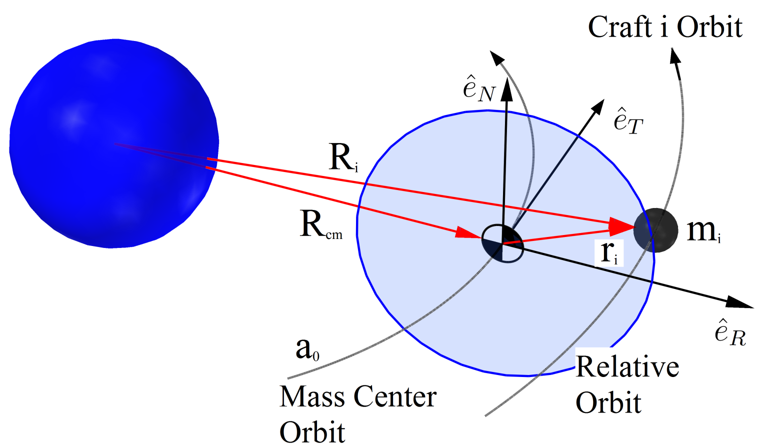


**Figure 1. Rotating Hill-Frame showing Relative Position Vector $\mathbf{r_i}$**

net charge $q_i$, has a position vector relative to the CM, denoted $\mathbf{r}_i$. The linearized Clohessy-Wiltshire-Hill gravitational model,[23] and a net Coulomb acceleration defined using the Debye-Hückel point-charge model[24] are then assumed. This electrostatic force model accounts for partial shielding of each potential, using a constant and finite $\lambda_d$, and $r_{ij} = \|\mathbf{r}_i - \mathbf{r}_j\|$ denotes the separation distance between crafts $i$ and $j$. This approximate model is demonstrated to be highly accurate, both experimentally and numerically, so long as all $r_{ij} > 10R_{sc}$ .[19,25] The acceleration of craft $i$ can then be written as in Eqs. (2b)-(2c), where $x$, $y$, and $z$ denote components along the axes: $\hat{e}_R$, $\hat{e}_T$, and $\hat{e}_N$, respectively. Also, gravitational terms are denoted $\mathbf{G}$, and Coulomb terms denoted $\mathbf{H}$. Charge products $Q_{ij} = q_i\, q_j$ are considered, often in this work, to be fully controllable/adjustable controls.

$$\sum_i m_i \mathbf{r}_i = 0 \tag{2a}$$

$$\ddot{\mathbf{r}}_i = \begin{bmatrix} \ddot{x}_i \\ \ddot{y}_i \\ \ddot{z}_i \end{bmatrix} = \mathbf{G}_i + \mathbf{H}_i \tag{2b}$$

$$\ddot{\mathbf{r}}_i = \begin{bmatrix} 2\omega \dot{y}_i + 3\omega^2 x_i \\ -2\omega \dot{x}_i \\ -\omega^2 z_i \end{bmatrix} + \left[ \frac{k_c \ q_i}{m_i} \sum_{j \neq i} \frac{q_j \ e^{-r_{ij}/\lambda_d}}{r_{ij}^3} \left(1 + \frac{r_{ij}}{\lambda_d}\right) \mathbf{r_{ij}} \right] \tag{2c}$$

### C. Linear Systems and Invariant Manifold Theory Overview

Any Coulomb formation may be written as a 1st order ODE system, which can be linearized about a reference state $\mathbf{X}^*$ to yield an ODE system that governs small state perturbations $\delta\mathbf{X}$, as shown in Eq. (3).

$$\dot{\mathbf{X}} = \mathbf{F}\left(\mathbf{X},\ \mathbf{u},\ t\right) \qquad \delta\dot{\mathbf{X}} = \left(\frac{\partial \mathbf{F}}{\partial \mathbf{X}}\right)\Bigg|_{\mathbf{X}^*} \delta\mathbf{X} = \mathbf{A}\ \delta\mathbf{X} \tag{3}$$

Where, $t$ is time, $\mathbf{X}$ is the state vector, and $\mathbf{u}$ contains the independent controls. Small state perturbations $\delta\mathbf{X}$ about some reference trajectory $\mathbf{X}^*$, are then governed by Eq. (3). The Jacobian matrix $\mathbf{A}$ of the linearized ODE system can be transformed to Jordan canonical form. In this way, the state perturbation vector $\delta\mathbf{X}$ may be decomposed into unstable, stable, and center eigenspaces ($E^u$, $E^s$, $E^c$ with dimensions $N_u$, $N_s$, and $N_c$, respectively).[26]

The global stable and unstable manifolds (if they exist) are subspaces containing all trajectories (or flows) governed by the original nonlinear system dynamics ($\mathbf{F}$), with the following properties:[26]

1. Unstable manifold ($W^u$): set of all trajectories which depart $\mathbf{X}^*$ asymptotically as $t \to \infty$.
2. Stable manifold ($W^s$): set of all trajectories which approach $\mathbf{X}^*$ asymptotically as $t \to -\infty$.
3. The manifolds are invariant, and therefore a state contained within $W^u$ or $W^s$ remains in that subspace for all time (e.g. $W^u \leftrightarrow W^s$ flows cannot occur).
4. The manifolds are tangent to their respective eigenspaces, in both $\pm$ directions at $\mathbf{X}^*$, and the $\pm$ yields two branches for $W^u$ and $W^s$. Also, the manifold subspaces are 1-D higher than their corresponding eigenspaces (i.e. $W^u$ has dimension of $N_u + 1$).

The manifolds are generated by initiating small maneuvers ($\Delta\mathbf{v}^{u/s} = \pm\epsilon\ E_{\mathbf{v}}^{u/s}$). Where, $E_{\mathbf{v}}^{u/s}$ indicates the velocity components of the normalized eigenvectors which span either $E^u$ or $E^s$, and $\epsilon$ is a small number. When constructing $W^u$, the perturbed states $\mathbf{X^u} = \mathbf{X}^* \pm \epsilon\ E_{\mathbf{v}}^u$ are propagated forward in time using $\mathbf{F}$; whereas, for $W^s$ the corresponding perturbed states are propagated backward in time.

## III. Three-Craft Collinear Coulomb Formation Existence

Berryman and Schaub[8] show that 3-craft collinear equilibrium only exist when the vehicles are aligned along a Hill-axis, and present necessary equilibria conditions, but without including plasma shielding. The equilibria conditions do not ensure real-valued charges (potentials), but a set of real equilibrium charges are known to exist for all Hill-axes and separation distances.[8] In this work, necessary and sufficient conditions are derived, with the inclusion of shielding, for the first time. The sufficient conditions establish bounds on the charge products to ensure non-imaginary values, and these bounds present discrete equilibria regions or cases. The stability properties of each of these regions are then analyzed, also for the first time.

A notation, introduced by Berryman and Schaub,[8] is adopted here to describe these 3-craft equilibria. Each craft is located on a single Hill-axis, and therefore a positive scalar $d_i$ denotes craft $i$ radial distance along that line (and $r_i$ denotes the signed distance). Since the craft numbering is arbitrary, it is assumed that: $r_1 = -d_1 < 0$ and $r_3 = d_3 > 0$, as illustrated in Figure 2.

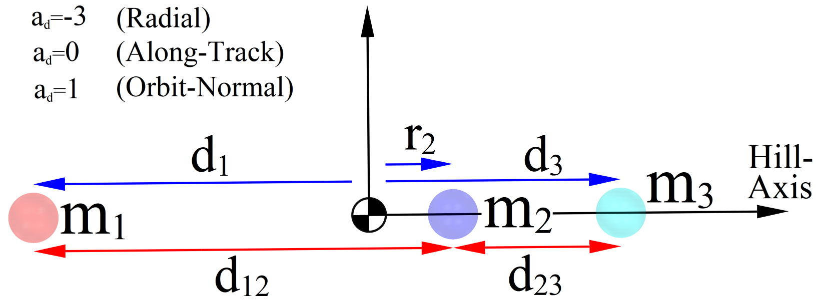


**Figure 2. Three-Craft Collinear Equilibrium Geometry and Notation**

Where, $d_{ij} = |r_{ij}| = |r_i - r_j|$ and the term $a_d$ is used to differentiate between the gravitational accelerations of the Radial ($\hat{e}_R$), Along-Track ($\hat{e}_T$), and Orbit-Normal ($\hat{e}_N$) aligned formations. The three scalar expressions of Eq. (4a) define the 3-craft collinear equilibria, using this notation. These are derived from Eqs. (2b)-(2c), with all time derivatives equal to zero, and with the substitution of a scaled charge product $\tilde{Q}_{ij}$, given by Eq. (4b).

$$a_d m_i r_i = \sum\nolimits_{j \neq i}^{3} \left( \frac{\tilde{Q}_{ij} \left(1 + \frac{d_{ij}}{\lambda_d}\right)}{d_{ij}^3 \; exp\left[d_{ij}/\lambda_d\right]} r_{ij} \right) \qquad i,j = 1 \ldots 3 \tag{4a}$$

$$\tilde{Q}_{ij} = \frac{k_c \; Q_{ij}}{\omega^2} \tag{4b}$$

One of the Eq. (4a) expressions is linearly dependent, and therefore there are a total of three conditions (including the CM constraint), and there are five unknowns: the three $\tilde{Q}_{ij}$, $d_1$, and $d_3$. To handle this under-determined system, Berryman and Schaub[8] specify $\tilde{Q}_{13}$, $d_1$ , and $d_3$ ($r_2$ known explicitly), and then compute $\tilde{Q}_{12}$ and $\tilde{Q}_{23}$ as functions of those quantities. This is also done here, but in addition, bounds on $\tilde{Q}_{13}$ are defined, which are sufficient to ensure real charges.

### A. Necessary Equilibrium Conditions with Shielding

Enforcing the assumed sign convention, shown in Figure 2, on the $r_i$ and $r_{ij}$ terms in Eq. (4a), and then solving $\tilde{Q}_{12}$ and $\tilde{Q}_{23}$, results in Eqs. (5a)-(5b). These are necessary conditions for three-craft collinear static equilibria, where the $\theta_{ij}$ terms account for shielding.

$$\tilde{Q}_{12} = \frac{1}{\theta_{12}} \left[a_d d_1 m_1 - \theta_{13} \tilde{Q}_{13}\right] \qquad \tilde{Q}_{23} = \frac{1}{\theta_{32}} \left[a_d d_3 m_3 - \theta_{13} \tilde{Q}_{13}\right] \tag{5a}$$

$$\theta_{ij} = \frac{[1 + d_{ij}/\lambda_d]}{d_{ij}^2 \; exp[d_{ij}/\lambda_d]} \tag{5b}$$

Throughout this work, scaled individual craft charges $\tilde{q}_i$ are computed using the Eq. (6) convention.

$$\tilde{q}_1 = \sqrt{\frac{\tilde{Q}_{12}\tilde{Q}_{13}}{\tilde{Q}_{23}}} \qquad \tilde{q}_2 = \frac{\tilde{Q}_{12}}{\tilde{q}_1} \qquad \tilde{q}_3 = \frac{\tilde{Q}_{13}}{\tilde{q}_1} \tag{6}$$

### B. Sufficient Conditions for Real Equilibrium with Shielding

An examination of Eqs. (5a)-(5b) for varying values of $d_3$, $d_1$ and $\tilde{Q}_{13}$, enable sufficient equilibria conditions (bounds on $\tilde{Q}_{13}$) to be defined. These conditions yield regions in the design space, outside of which equilibria cannot exist, and these are presented on a case by case basis as follows:

1. **Along-Track** ( $\tilde{Q}_{13} > 0$ )
   Equilibria exist for all: $\tilde{Q}_{13} > 0$, $d_1$, and $d_3$.

2. **Orbit-Normal**
   - **Case A:** ( $\tilde{Q}_{13} > 0$, $\tilde{Q}_{12} > 0$, and $\tilde{Q}_{23} > 0$ )
     Equilibria exist so long as: $\tilde{Q}_{13} < m_1 d_1/\theta_{13}$ and $\tilde{Q}_{13} < m_3 d_3/\theta_{13}$.
   - **Case B:** ( $\tilde{Q}_{13} > 0$, $\tilde{Q}_{12} < 0$, and $\tilde{Q}_{23} < 0$ )
     Equilibria exist so long as: $\tilde{Q}_{13} > m_1 d_1/\theta_{13}$ and $\tilde{Q}_{13} > m_3 d_3/\theta_{13}$.

3. **Radial**
   - **Case A:** ( $\tilde{Q}_{13} > 0$, $\tilde{Q}_{12} < 0$, and $\tilde{Q}_{23} < 0$ )
     Equilibria exist for all: $\tilde{Q}_{13} > 0$, $d_1$, and $d_3$.
   - **Case B:** ( $\tilde{Q}_{13} < 0$, $\tilde{Q}_{12} < 0$, and $\tilde{Q}_{23} > 0$ )
     Equilibria exist for $d_1 > d_3$ ($r_2 > 0$), and so long as: $|\tilde{Q}_{13}| > 3m_3 d_3/\theta_{13}$ and $|\tilde{Q}_{13}| < 3m_1 d_1/\theta_{13}$. Therefore, $|\tilde{Q}_{13}|$ is bounded above and below based on the values of $d_1$ and $d_3$.
   - **Case C:** ( $\tilde{Q}_{13} < 0$, $\tilde{Q}_{12} > 0$, and $\tilde{Q}_{23} < 0$ )
     Equilibria exist for $d_1 < d_3$ ($r_2 < 0$), and so long as: $|\tilde{Q}_{13}| < 3m_3 d_3/\theta_{13}$ and $|\tilde{Q}_{13}| > 3m_1 d_1/\theta_{13}$. Again $|\tilde{Q}_{13}|$ is bounded above and below.

Feasible $\tilde{Q}_{13}$ is finite and bounded for both Orbit-Normal cases and for Radial cases B-C. As such, a feasible $\tilde{Q}_{13}$, as a function of $d_1$ and $d_3$, may be defined using Eqs. (7a)-(7c). This only ensures a feasible equilibrium and does not necessarily provide ideal charges or optimization of any sort.

$$\sigma_L = \min\left(\left|\frac{a_d m_1 d_1}{\theta_{13}}\right|, \left|\frac{a_d m_3 d_3}{\theta_{13}}\right|\right) \qquad \sigma_U = \max\left(\left|\frac{a_d m_1 d_1}{\theta_{13}}\right|, \left|\frac{a_d m_3 d_3}{\theta_{13}}\right|\right) \tag{7a}$$

$$\text{Orbit-Normal Case A:} \quad \tilde{Q}_{13} = \sigma_L/2 \qquad \text{Orbit-Normal Case B:} \quad \tilde{Q}_{13} = 1.01\ \sigma_U \tag{7b}$$

$$\text{Radial Cases B-C:} \quad \tilde{Q}_{13} = -\left(\frac{\sigma_L + \sigma_U}{2}\right) \tag{7c}$$

In addition, trivial cases where $\tilde{Q}_{12} = \tilde{Q}_{23} = q_2 = 0$ ($r_2 = 0$) can also be derived from Eq. (5a). These cases, defined by Eq. (8), are considered trivial because they simply reduce to the 2-craft Hill-Frame configurations (along each axis).

$$\tilde{Q}_{13} = \frac{a_d m_1 d_1}{\theta_{13}} = \frac{a_d m_3 d_3}{\theta_{13}} \qquad d_1 = \frac{m_3 d_3}{m_1} \tag{8}$$

The only technical difference from the 2-craft cases, is the addition of a non-interacting craft (craft 2), which is located at the CM (origin). The 2-craft equilibria and their respective stability properties are examined in detail by, among others: Jones,[20] Natarajan and Schaub,[27] and Inampudi.[16]

# IV. Three-Craft Collinear Equilibrium Stability Analysis

Each of the equilibrium regions presented in Section III-B have distinct eigenspaces and stability properties; however, all are dynamically unstable. These differences lead to varied unstable and stable manifold structures which are demonstrated and discussed here. The relative instability and the properties of eigenvector modes are especially important to the design of feedback stabilization strategies.

### A. Linearized Eigenspace Properties

In deriving the linearized ODE system as in Eq. (3), craft 2 is removed via the CM condition, reducing the system dimension from 18 to 12. The eigenspaces and invariant manifolds are numerically computed using the Eq. (2c) dynamics with $\lambda_d = 180$ m, and for equal mass craft $m_1 = m_2 = m_3 = m = 150$ kg, and $a_0 = 4.227e^7$ m. Also, $\tilde{Q}_{13} = 1.0e^4$ is selected, or for Orbit-Normal and Radial cases B-C it is calculated using Eqs. (7a)-(7c). The eigenspaces for all cases are described as follows:

1. **Along-Track**

   $N_u = N_s = 1$ (distinct real) - Mode is contained in the $\hat{e}_R$-$\hat{e}_T$ plane. Perturbations along $\hat{e}_N$ only are marginally stable.

2. **Orbit-Normal Case A:**

   $N_u = N_s = 4$ (2 complex pairs) - All unstable/stable modes are contained in the $\hat{e}_R$-$\hat{e}_T$ plane, and therefore perturbations along $\hat{e}_N$ only are marginally stable.

3. **Orbit-Normal Case B:**

   $N_u = N_s = 3$ (1 complex pair, 1 mode real) - The complex mode is contained in the $\hat{e}_R$-$\hat{e}_T$ plane.

   - $|d_1 - d_3|$ Small: Real mode is contained in the $\hat{e}_R$-$\hat{e}_T$ plane. Perturbations along $\hat{e}_N$ only are marginally stable.
   - $|d_1 - d_3|$ Large: Real mode is entirely along $\hat{e}_N$. Perturbations along $\hat{e}_N$ only are unstable.

4. **Radial Case A:**

   $N_u = N_s = 2$ (2 distinct real) - Both modes are contained in the $\hat{e}_R$-$\hat{e}_T$ plane, and perturbations along $\hat{e}_N$ only are marginally stable.

5. **Radial Cases B-C:**

   - $|d_1 - d_3|$ Small: $N_u = N_s = 3$ (1 complex pair, 1 real) - All modes are contained in the $\hat{e}_R$-$\hat{e}_T$ plane. Perturbations along $\hat{e}_N$ only are marginally stable.
   - $|d_1 - d_3|$ Large: $N_u = N_s = 3$ (3 distinct real) - Two modes are contained in the $\hat{e}_R$-$\hat{e}_T$ plane, and the other mode is entirely along $\hat{e}_N$. Perturbations along $\hat{e}_N$ only are unstable.

In this analysis, there are no stability bifurcations (changes to $N_u$ or $N_s$), within each case, as a function of $d_1$, $d_3$, and $\tilde{Q}_{13}$. Moreover, no bifurcations occur as $\lambda_d \to \infty$ (no shielding) for all cases except for the Along-Track, which bifurcates to $N_u = N_s = 0$ (all distinct eigenvalues). What is particularly interesting in this analysis is the differing out-of orbit-plane ($\hat{e}_N$) stability for the Orbit-Normal case B and Radial cases B-C, as a function of $|d_1 - d_3|$. This observation is especially important, because it demonstrates that marginal out-of-plane stability for the Radial configuration (and along-line marginal stability for Orbit-Normal) can be achieved through careful selection of the distances $d_1$ and $d_3$, and the charge product $\tilde{Q}_{13}$. This stability property and the conditions under which it arises was until now unknown. For either axis of alignment, the $\hat{e}_N$ instabilities arise when two craft are in close-proximity and have a repulsive Coulomb force which becomes larger than the restorative differential gravity force. Therefore, the appearance of this instability depends on $|d_1 - d_3|$, as well as $\tilde{Q}_{ij}$ magnitudes.

### B. Explanation of Radial Configuration $\hat{e}_N$ Instabilities

All Radial configuration cases exhibit at least one Coulomb force magnitude that is on the order of differential gravity. For case A, there are attractive forces between inner-craft and a repulsive force between the outer-craft, and the attractions are many magnitudes larger than the repulsion. For cases B-C, the two craft in closest proximity have the repulsive force, and all forces are similar in magnitude. Force diagrams for both cases are presented in Figures 3(a)-3(b), where a larger arrow thickness indicates a larger force magnitude.[a] For case A, any out-of-plane perturbations ($z$ components) are quickly restored by the strong inner-craft forces. Whereas for case B, perturbations can cause the repulsive force acting on craft 2 to dominate the

[a] In Figures 3(a)-3(b) and all subsequent figures, S/C is used as a shorthand for spacecraft.

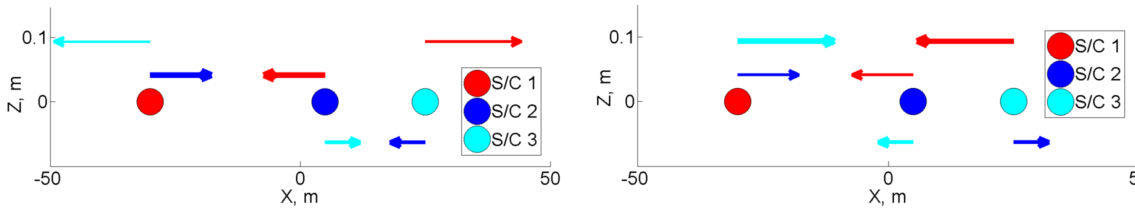


(a) Case A (b) Case B

**Figure 3. 3-Craft Radial Configuration Force Diagrams**

restorative forces, and can cause its $z$ component to increase further. This occurs when $d_{23}$ is small ($|d_1 - d_3|$ large), and when $\tilde{Q}_{23}$ is large enough. The resulting $\hat{e}_N$ perturbations destabilize the in-plane forces, but as craft distances increase, differential gravity begins to dominate and the $\hat{e}_N$ perturbations remain bounded.

### C. Orbit-Normal Along-Line Marginal Stability

The case A unstable/stable eigenvectors do not have $\hat{e}_N$ components, whereas one of the case B unstable/stable modes is entirely in the $\hat{e}_N$ direction, when $|d_1 - d_3|$ is sufficiently large. Therefore, case A Orbit-Normal configurations are marginally stable along the $\hat{e}_N$ direction, which decouples to 1st order. This property was known for the 2-craft Orbit-Normal equilibrium, but until now it was unknown that the 3-craft configuration could share this along-line stability. This difference is apparent by analyzing the force diagrams shown in Figures 4(a)-4(b). The case A configuration has all repulsive forces, and therefore any contraction of the formation will be repelled, and formation expansion will be countered by differential gravity. In contrast, the case B configuration has attractive forces between inner-craft, and therefore contraction perturbations between those vehicles will grow, eventually leading to potential collisions. This is important,

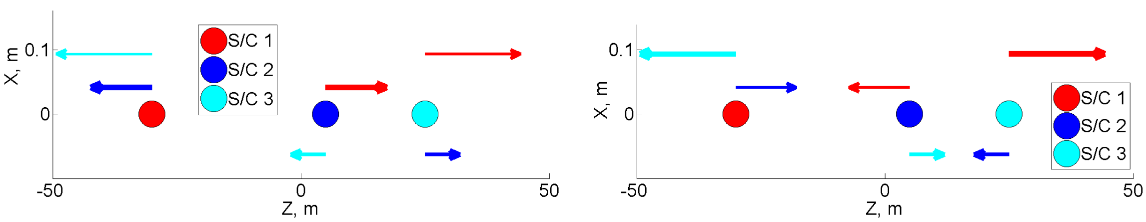


(a) Case A (b) Case B

**Figure 4. 3-Craft Orbit-Normal Force Diagrams**

because so long as $d_1$, $d_3$, and $\tilde{Q}_{13}$ are selected properly, substantial control effort need only be applied to attitude perturbations. This property is realized by Natarajan and Schaub,[15] for the 2-craft configuration, where the linearized separation distance is shown to represent a stable, simple harmonic oscillator. Numerical simulation verifies that 3-craft Orbit-Normal configurations can share this facet.

## V. Invariant Manifolds for the Three-Craft Collinear Equilibria

Invariant manifolds are analyzed to illustrate some of the previously presented stability properties, but also to understand how natural motions may be best exploited to aid in reconfiguring the formations. Reconfigurations of interest include: expansions and contractions of the overall distance $d_{13}$, transfers between equilibrium regions, and transfers between one axis of alignment to another. Moreover, the manifolds could be used in order to expel or add a craft by transferring between a 2-craft equilibrium and a 3-craft equilibrium (with one craft leaving or entering the system).

The linearized ODE systems and assumptions of Section IV are used in all numerically generated invariant manifolds which follow. The manifolds are initiated with a $\Delta\mathbf{v}$ perturbation (for each craft) along the associated eigenspace vectors, with $\epsilon = 0.1$ mm/sec. Also, it is known that all Orbit-Normal and Radial cases B-C (for $|d_1 - d_3|$ large) unstable/stable manifolds are in $\Re^6$, whereas the remaining cases are in $\Re^4$, since modal motion is confined to the $\hat{e}_R$-$\hat{e}_T$ plane. Radial case A unstable manifolds are illustrated in Figure 5(a) which shows that motion is confined to the reference orbit-plane. There is strong attractive Coulomb interaction between 2 of the inner-craft on each branch, which makes the trajectories have many intersections. Figure 5(b) demonstrates the out-of-plane instability for case B, resulting in a $\Re^3$ (in position) manifold structure. On one branch, the attractive forces bring all vehicles together, which in turn, increases

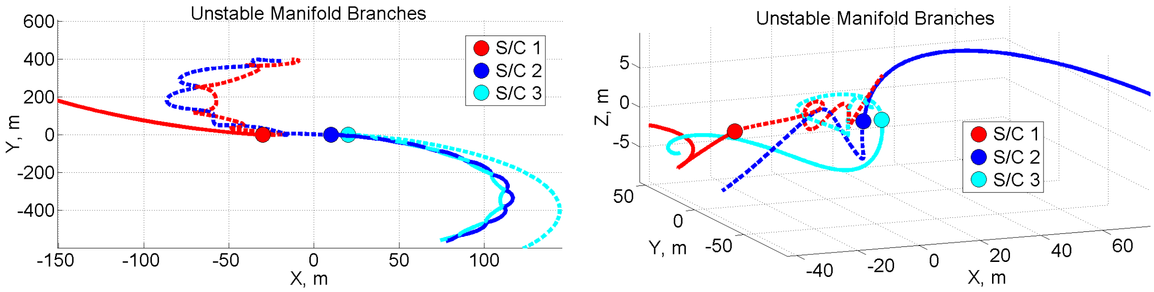


(a) Case A: 1.0 $T_p$, $d_3 = 25$ m, and $\tilde{Q}_{13} = 1.0e^4$ (b) Case B: 0.5 $T_p$, $d_3 = 18$ m, and $\tilde{Q}_{13} = -2.56e^7$

**Figure 5. 3-Craft Radial Unstable Manifolds for $d_1 = 30$ m**

the repulsive force on craft 2, thereby giving it an increasing $z$ component. On the other branch, the repulsive force on craft 2 causes it to move away from the other two craft. For both branches, the purely real $\hat{e}_N$ unstable mode is quite distinct.

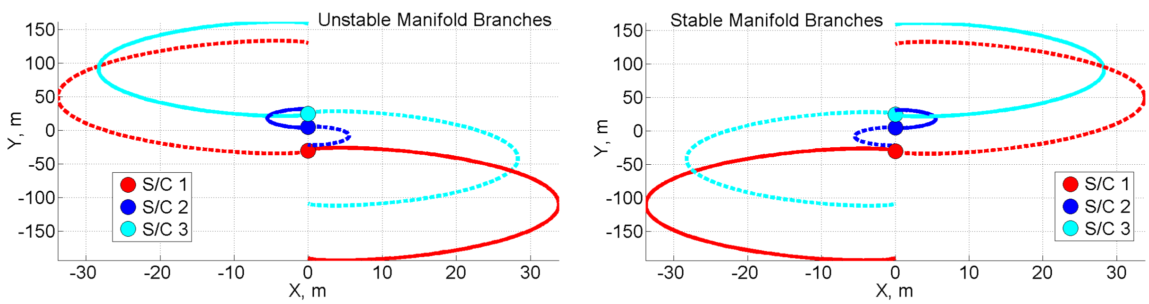


(a) Unstable (b) Stable

**Figure 6. 3-Craft Along-Track Invariant Manifolds for:** 1.0 $T_p$**,** $d_1 = 30$ **m,** $d_3 = 25$ **m, and** $\tilde{Q}_{13} = 1.0e^4$

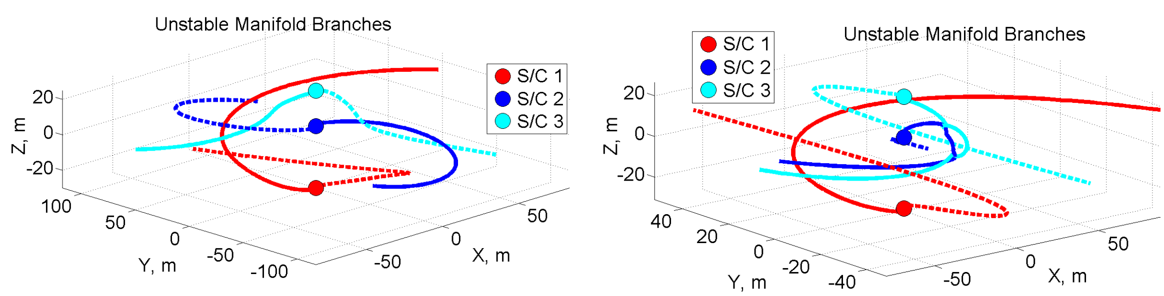


(a) Case A: $\tilde{Q}_{13} = 5.9e^6$ (b) Case B: $\tilde{Q}_{13} = 1.43e^7$

**Figure 7. 3-Craft Orbit-Normal Unstable Manifolds for:** 1.0 $T_p$**,** $d_1 = 30$ **m,** $d_3 = 25$ **m,**

Next, Along-Track stable and unstable manifolds are illustrated in Figures 6(a)-6(b). There is great symmetry between stable and unstable branches, and it is rather intuitive to visualize a transfer trajectory from unstable to stable manifolds, which could expand or contract this formation with little control effort. Finally, some Orbit-Normal unstable manifolds are illustrated in Figures 7(a)-7(b). The case A manifolds resemble the 2-craft Orbit-Normal manifolds, which also exhibit along-line marginal stability. The case B manifolds have strong Coulomb interaction between craft 2 and 3, because of their attractive force. It is this attraction which can cause the $\hat{e}_N$ unstable mode for that case.

### A. Reconfigurations between Three-Craft Collinear Equilibria along Manifolds

As mentioned previously, expansions and contractions between Along-Track configurations are relatively intuitive to visualize. Figure 8 demonstrates an example initial guess (IG) trajectory which would expand the Along-Track configuration, increasing $d_{13}$ by 10 meters and also moving $r_2$ from +5 meters to +3 meters. This is an IG only, because there are state discontinuities between unstable and stable manifolds at the patch

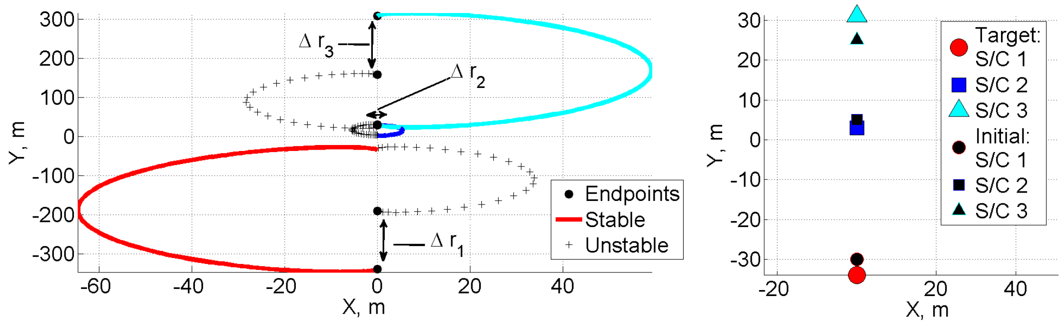


**Figure 8. Along-Track Initial Guess Expansion Trajectory along Invariant Manifolds: $d_1 = 30 \rightarrow 36$ m, $d_3 = 25 \rightarrow 34$ m, Both Manifolds Propagated 1 $T_p$**

point (endpoints of near manifold intersection on plot). Nevertheless, it is likely that these discontinuities could be differentially corrected, to yield a continuous transfer with little control effort, as demonstrated by Jones and Schaub[20,21] for 2-craft Hill-Frame equilibria, where $\Delta V$ was minimized.

Another IG expansion example, is illustrated in Figure 9 for the Orbit-Normal case A configuration, and for an increased $d_{13}$ of 20 m ($r_2$ constant). This transfer is more difficult to visualize because it is

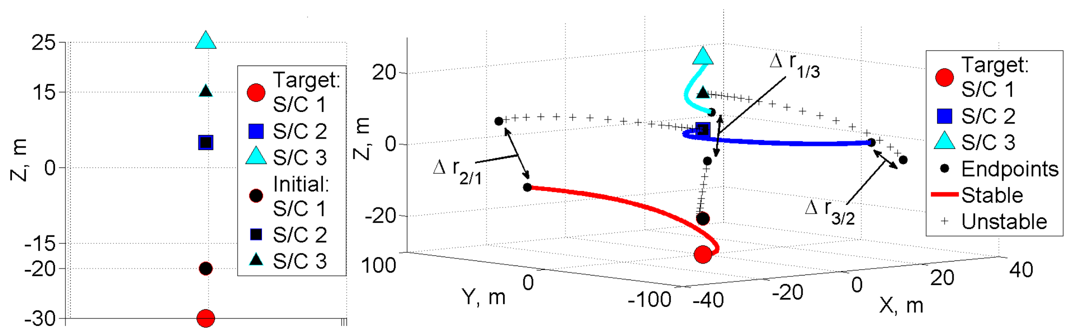


**Figure 9. Orbit-Normal Initial Guess Expansion Trajectory along Invariant Manifolds: $d_1 = 20 \rightarrow 30$ m, $d_3 = 15 \rightarrow 25$ m, Both Manifolds Propagated 0.7 $T_p$**

$\Re^3$ (in position), and because the velocity directions are hard to ascertain. In addition, for expansions of this configuration, the manifolds are best exploited when the spacecraft numbering changes. Therefore, in Figure 9 craft 1 moves to $d_3$ slot, craft 2 to $d_1$, and craft 3 to $r_2$. This is completely reasonable, assuming equal mass craft, but discontinuities of charge at the patch point could be large. These initial trajectories introduce the possibility of extending the previously developed method for converging fuel-optimal reconfigurations,[20,21] to the 3-craft collinear formations.

The Radial configuration manifolds are not as readily useful to aid in contraction and expansion transfers. Fortunately, these configurations turn out to be fully controllable in the $\hat{e}_R - \hat{e}_T$ plane using only charge control, as demonstrated in Section VI. This means that charge control alone can be used to maintain, expand, and contract these cases, and therefore using manifolds to reduce inertial thrust cost is unnecessary.

# VI. Three-Craft Collinear Formation: Orbit-Plane Feedback Stabilization

The Along-Track and Radial configurations, which have unstable/stable manifolds contained in the $\hat{e}_R$-$\hat{e}_T$ plane (reference orbit plane), are considered here. These exhibit marginal out-of orbit-plane stability, and therefore a reduced system controller is designed, considering only planar $\hat{e}_R$-$\hat{e}_T$ dynamics. An initial controller is developed assuming: Debye shielding is negligible, all craft have equal mass ($m = 150$ kg), and craft 2 dynamics are explicitly removed via the CM constraint. These conditions are enforced, and scaled charge products $\tilde{Q}_{ij}$, defined by Eq. (4b), are substituted into the $\hat{e}_R$-$\hat{e}_T$ terms of Eq. (2c). This yields scaled craft 1 and 3 accelerations, given by Eqs. (9a)-(9b).

$$\frac{\ddot{\mathbf{r}}_1}{\omega^2} = \mathbf{r}_1'' = \frac{1}{\omega^2}\begin{bmatrix} \ddot{x}_i \\ \ddot{y}_i \end{bmatrix} = \begin{bmatrix} 2\dot{y}_1/\omega + 3x_1 \\ -2\dot{x}_1/\omega \end{bmatrix} + \frac{\tilde{Q}_{13}}{m\ d_{13}^3}\begin{bmatrix} x_1 - x_3 \\ y_1 - y_3 \end{bmatrix} + \frac{\tilde{Q}_{12}}{m\ d_{12}^3}\begin{bmatrix} 2\ x_1 + x_3 \\ 2\ y_1 + y_3 \end{bmatrix} \tag{9a}$$

$$\frac{\ddot{\mathbf{r}}_3}{\omega^2} = \mathbf{r}_3'' = \frac{1}{\omega^2}\begin{bmatrix} \ddot{x}_3 \\ \ddot{y}_3 \end{bmatrix} = \begin{bmatrix} 2\dot{y}_3/\omega + 3x_3 \\ -2\dot{x}_3/\omega \end{bmatrix} + \frac{\tilde{Q}_{13}}{m\ d_{13}^3}\begin{bmatrix} x_3 - x_1 \\ y_3 - y_1 \end{bmatrix} + \frac{\tilde{Q}_{23}}{m\ d_{12}^3}\begin{bmatrix} 2\ x_3 + x_1 \\ 2\ y_3 + y_1 \end{bmatrix} \tag{9b}$$

Where, the substitution of the scaled charge products has introduced a time transformation into the equations of motion, as defined by Eq. (10). This transform to the variable $\tau$ reduces numerical integration error, and helps to prevent poor scaling of the linearized dynamics' matrices.

$$d\tau = \omega dt \qquad (\zeta)' = \frac{d\zeta}{d\tau} = \frac{1}{\omega}\frac{d\zeta}{dt} \tag{10}$$

Next, Eqs. (9a)-(9b) are linearized about the equilibrium state $\mathbf{X}^*$, yielding a time-invariant, controlled system, defined in general state-space form by Eq. (11). The matrices $\mathbf{A}$ and $\mathbf{B}$ are given explicitly for the Radial configuration by Eqs. (12a)-(12b), where $\tilde{Q}_{ij}^*$ ($\tilde{q}_i^*$), $d_{ij}$ , and $r_i$ denote equilibrium: scaled charge products (scaled charges), separation distances, and signed distances, respectively.

$$\delta\mathbf{X}' = \mathbf{A}\ \delta\mathbf{X} + \mathbf{B}\ \mathbf{u} \qquad \delta\mathbf{X} = \begin{bmatrix} \delta\mathbf{r}_1 \\ \delta\mathbf{r}_3 \\ \delta\mathbf{v}_1 \\ \delta\mathbf{v}_3 \end{bmatrix}_{8x1} \qquad \mathbf{u} = \begin{bmatrix} \delta q_1 \\ \delta q_2 \\ \delta q_3 \end{bmatrix}_{3x1} \tag{11}$$

$$\mathbf{A} = \begin{bmatrix} 0 & 0 & 0 & 0 & 1 & 0 & 0 & 0 \\ 0 & 0 & 0 & 0 & 0 & 1 & 0 & 0 \\ 0 & 0 & 0 & 0 & 0 & 0 & 1 & 0 \\ 0 & 0 & 0 & 0 & 0 & 0 & 0 & 1 \\ 3 - \frac{4\tilde{Q}_{12}^*}{md_{12}^3} - \frac{2\tilde{Q}_{13}^*}{md_{13}^3} & 0 & -\frac{2\tilde{Q}_{12}^*}{md_{12}^3} + \frac{2\tilde{Q}_{13}^*}{md_{13}^3} & 0 & 0 & 2 & 0 & 0 \\ 0 & \frac{2\tilde{Q}_{12}^*}{md_{12}^3} + \frac{\tilde{Q}_{13}^*}{md_{13}^3} & 0 & \frac{\tilde{Q}_{12}^*}{md_{12}^3} - \frac{\tilde{Q}_{13}^*}{md_{13}^3} & -2 & 0 & 0 & 0 \\ -\frac{2\tilde{Q}_{23}^*}{md_{23}^3} + \frac{2\tilde{Q}_{13}^*}{md_{13}^3} & 0 & 3 - \frac{4\tilde{Q}_{23}^*}{md_{23}^3} - \frac{2\tilde{Q}_{13}^*}{md_{13}^3} & 0 & 0 & 0 & 0 & 2 \\ 0 & \frac{\tilde{Q}_{23}^*}{md_{23}^3} - \frac{\tilde{Q}_{13}^*}{md_{13}^3} & 0 & \frac{2\tilde{Q}_{23}^*}{md_{23}^3} + \frac{\tilde{Q}_{13}^*}{md_{13}^3} & 0 & 0 & -2 & 0 \end{bmatrix} \tag{12a}$$

$$\mathbf{B} = \begin{bmatrix} \mathbf{0}_{4x1} & \mathbf{0}_{4x1} & \mathbf{0}_{4x1} \\ \frac{|\tilde{q}_1^*|\tilde{q}_2^*(2r_1+r_3)}{md_{12}^3} + \frac{|\tilde{q}_1^*|\tilde{q}_3^*(r_1-r_3)}{md_{13}^3} & \frac{|\tilde{q}_2^*|\tilde{q}_1^*(2r_1+r_3)}{md_{12}^3} & \frac{|\tilde{q}_3^*|\tilde{q}_1^*(r_1-r_3)}{md_{13}^3} \\ 0 & 0 & 0 \\ \frac{|\tilde{q}_1^*|\tilde{q}_3^*(r_3-r_1)}{md_{13}^3} & \frac{|\tilde{q}_2^*|\tilde{q}_3^*(2r_3+r_1)}{md_{23}^3} & \frac{|\tilde{q}_3^*|\tilde{q}_2^*(2r_3+r_1)}{md_{23}^3} + \frac{|\tilde{q}_3^*|\tilde{q}_1^*(r_3-r_1)}{md_{13}^3} \\ 0 & 0 & 0 \end{bmatrix} \tag{12b}$$

Where, the $|\tilde{q}_i^*|$ are added as scaling parameters to ensure that the $\mathbf{B}$ matrix has terms with equal order of magnitude and on the order of terms in $\mathbf{A}$. This numerical scaling is crucial in successfully computing feedback gains numerically. Also, using the individual charges as opposed to the charge products ensures that real-values are maintained during control operation. With this scaling, the craft charges are given by Eq. (13), where $\mathbf{K}$ is a $3x8$ full-state feedback gain matrix.

$$\begin{bmatrix} \tilde{q}_1(\tau) \\ \tilde{q}_2(\tau) \\ \tilde{q}_3(\tau) \end{bmatrix} = \begin{bmatrix} \tilde{q}_1^* \\ \tilde{q}_2^* \\ \tilde{q}_3^* \end{bmatrix} + \begin{bmatrix} |\tilde{q}_1^*|\ \delta q_1(\tau) \\ |\tilde{q}_2^*|\ \delta q_2(\tau) \\ |\tilde{q}_3^*|\ \delta q_3(\tau) \end{bmatrix} \qquad \mathbf{u} = \begin{bmatrix} \delta q_1(\tau) \\ \delta q_2(\tau) \\ \delta q_3(\tau) \end{bmatrix} = -\mathbf{K}\ \delta\mathbf{X}(\tau) \tag{13}$$

The Along-Track and all Radial cases have linearized systems which are fully controllable, made possible because of the coupling between $x$ and $y$ perturbations in the $\mathbf{A}$ matrix.[28] In contrast, the Orbit-Normal configurations are not fully controllable in the $\hat{e}_R$-$\hat{e}_T$ plane, and therefore some inertial thrusting would be required to maintain them. Moreover, it is demonstrated here, for the first time, that Radial case A $\hat{e}_R$-$\hat{e}_T$ planar perturbations can be asymptotically stabilized, using only charge control (no inertial thrust). An analogous result is demonstrated by Natarajan and Schaub,[27] for the Radial 2-craft configuration. From the state-space model of Eqs. (12a)-(12b), the gain matrix $\mathbf{K}$ is determined by solving the standard Linear-Quadratic Regulator (LQR) problem.[28]

### A. Radial Feedback Controller: Numerical Simulations

For the presented simulations, the LQR weighting matrices $\mathbf{Q}$ and $\mathbf{R}$ are both set to identity. The Coulomb configurations are numerically integrated using the nonlinear equations of motion given by Eqs. (9a)-(9b). Also, the same values for $m$, $a_0$, and $\tilde{Q}_{13}$ used in Section IV (and in generating the manifolds) are used here, for a nominal configuration of: $d_1 = 30$ m and $d_3 = 25$ m. Figures 10(a)-10(b) illustrate position perturbation and charge control histories after an initial $\Delta\mathbf{v}$ to crafts 1 and 3, with equal $x$ and $y$ components of 0.01 mm/s. Next, Figures 11(a)-11(b) show these histories, but for initial disturbances in position to all three craft, thereby demonstrating additional robustness in the control.

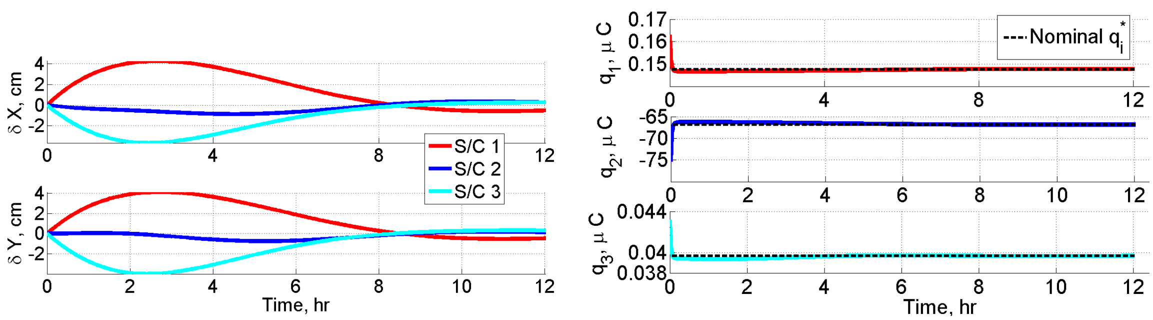


(a) Position Perturbations (b) Charge History

**Figure 10. Radial Case A: Planar Response and Control for Initial Δv Perturbations to S/C 1 and 3**

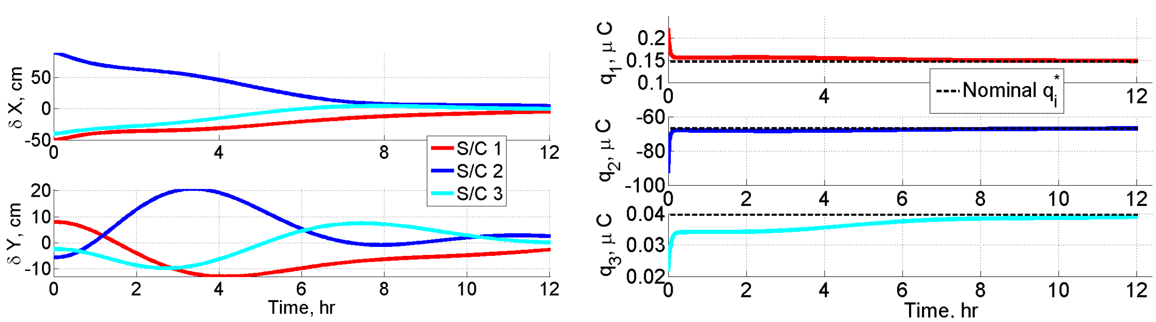


(a) Position Perturbations (b) Charge History

**Figure 11. Radial Case A: Planar Response and Control for Initial Δr Perturbations to all S/C**

The initial position perturbations for Figures 11(a)-11(b) are: $\Delta x_1 = -0.5$ m, $\Delta x_2 = 0.18$ m, $\Delta x_3 = 0.32$ m, $\Delta y_1 = 0.08$ m, $\Delta y_2 = -0.056$ m, and $\Delta y_3 = -0.024$ m. Note that the required nominal charge levels for this Radial equilibria are very small, $\mu C$ order, and the control variations in the charges required to remove the initial disturbances are relatively small. The nominal charge magnitudes and charge variation magnitudes are very feasible. In fact, the maximum power would be around 80 W, for $R_{sc} = 1$ m, and with sufficient current to overcome the incoming plasma current.

### B. Radial Feedback Controller with Plasma Shielding

Because there are no bifurcations in the Radial configuration eigenspace as function of $\lambda_d$, the controller methodology is easily altered to include shielding. For brevity, the linearized matrices **A** and **B** with plasma shielding included (and simulation results) are omitted; however, it is verified in numerical simulation that small planar perturbations can still be asymptotically stabilized. Also, it has been verified that small deviation in craft masses (including unequal masses) can be accommodated by this methodology. Nevertheless, this control design is preliminary, and therefore relaxing the assumptions used and improving robustness would be necessary prior to implementation. Specifically, the controlled response characteristics could be refined, to achieve desired performance, by tuning the LQR weighting matrices.

### C. Along-Track Feedback Control

Natarajan showed that there are no real-valued gains which can be used to stabilize 2-craft Along-Track Coulomb formations, thereby necessitating some inertial thrusting.[19] In contrast, the 3-craft Along-Track configuration does satisfy the linear controllability condition; however, it is very nearly uncontrollable numerically, and highly sensitive to perturbations. This system is said to be nearly uncontrollable, by computing a measure of the distance to an uncontrollable state-space system using the method of Boley and Lu.[29] The measure is small for the Along-Track, but relatively large for the Radial cases. These difficulties make a charge-only controller impractical, and perhaps even impossible, for the Along-Track formation. A coordinate change in the dynamics or the adoption of a nonlinear controller might alleviate some of these difficulties, otherwise a hybrid control would be necessary to stabilize this formation.

## VII. Conclusions

Necessary and sufficient conditions which enable, 3-craft collinear, static formations are derived in the presence of a linearized gravity model, and with the inclusion of partial Coulomb force shielding. A detailed stability analysis for each of the resulting equilibrium is carried out, which demonstrates that marginal stability, normal to the orbit-plane, can be achieved, although it is not assured for all cases. Furthermore, numerical simulation proves that a linearized charge feedback law (without inertial thrusting) is capable of asymptotically stabilizing in-plane perturbations, for the Radial configuration. These results were previously unknown, and demonstrate how the dynamical properties of these systems may be utilized to reduce station-keeping control effort. Control laws to stabilize the remaining 3-craft collinear configurations are lacking, but this paper presents stability and controllability properties for these cases, which suggest that some inertial thrusting will be required. Further work should focus on these challenges, as well as improve the robustness of the Radial configuration control law, relax some of the assumptions used, and possibly incorporate nonlinear control. Lastly, prominent continuous disturbances, such as solar radiation pressure, should be tested to validate the control designs.

Invariant manifold theory is applied to all equilibrium configurations, and examples are given which illustrate possible scenarios in which the manifolds may be exploited to reduce the cost associated with reshaping these formations. This analysis suggests that a previously demonstrated methodology for targeting minimal $\Delta V$ transfers between 2-craft Coulomb equilibria, along manifolds, can be applied to the 3-craft configurations as well. Future research will continue to investigate initial trajectories where unstable manifold flows nearly intersect stable flows, and thereby lend themselves to differential correction to match continuity. Such reconfigurations realize the advantageous property of Coulomb formations to change shape using charge control, preferably with as little inertial thrusting as possible.

## Acknowledgments

This research was made with Government support under and awarded by the Department of Defense (DoD) through the National Defense Science and Engineering Graduate (NDSEG) Fellowship Program.

## References

[1]Cover, J. H., Knauer, W., and Maurer, H. A., "Lightweight Reflecting Structures Utilizing Electrostatic Inflation," US Patent 3,546,706, October 1966.

[2]King, L., Parker, C., Deshmukh, S., and Chong, J., "Spacecraft Formation-flying Using Inter-vehicle Coulomb Forces," Tech. rep., NASA Institute for Advanced Concepts, January 2002.

[3]King, L., Parker, C., Deshmukh, S., and Chong, J., "Study of Interspacecraft Coulomb Forces and Implications for Formation Flying," *Journal of Propulsion and Power*, Vol. 19, No. 3, 2003, pp. 497–505.

[4]Lawson, P. and Dooley, J., "Technology Plan for the Terrestrial Planet Finder Interferometer," Tech. Rep. 05-5, NASA Jet Propulsion Lab, June 2005.

[5]Mullen, E., Gussenhoven, M., and Hardy, D., "SCATHA," *Journal of the Geophysical Sciences*, Vol. 91, No. A2, 1986, pp. 1474–1490.

[6]Whipple, E. and Olsen, R., "Importance of Differential Charging for Controlling Both Natural and Induced Vehicle Potentials on ATS-5 and ATS-6," *Proceedings of the 3rd Spacecraft Charging Technology Conference*, 1980, pp. 888–893.

[7]Escoubet, C., Fehringer, M., and Goldstein, M., "The Cluster Mission," *Annales Geophysicae*, Vol. 19, No. 10/12, 2001, pp. 1197–1200.

[8]Berryman, J. and Schaub, H., "Analytical Charge Analysis for Two- and Three-Craft Coulomb Formations," *Journal of Guidance, Control, and Dynamics*, Vol. 30, No. 6, 2007, pp. 1701–1710.

[9]Hussein, I. I. and Schaub, H., "Stability and Control of Relative Equilibria for the Three-Spacecraft Coulomb Tether Problem," *Acta Astronautica*, Vol. 65, No. 5–6, 2009, pp. 738–754.

[10]Hogan, E. and Schaub, H., "Collinear Invariant Shapes for Three-Craft Coulomb Formations," *AIAA/AAS Astrodynamics Specialists Conference*, No. 10-7954, August 2010, Toronto, ON.

[11]Wang, S. and Schaub, H., "Nonlinear Charge Control for a Collinear Fixed Shape," *AIAA/AAS Astrodynamics Specialists Conference*, No. 10-7955, August 2010, Toronto, ON.

[12]Schaub, H. and Hussein, I. I., "Stability and Reconfiguration Analysis of a Circulary Spinning Two-Craft Coulomb Tether," *IEEE Transactions on Aerospace and Electronic Systems*, Vol. 46, No. 4, October 2010, pp. 1675–1686.

[13]Hogan, E. and Schaub, H., "Linear Stability and Shape Analysis of Spinning Three-Craft Coulomb Formations," *Celestial Mechanics and Dynamical Astronomy*, Vol. 112, No. 2, 2012, pp. 131–148.

[14]Schaub, H. and Kim, M., "Orbit Element Difference Constraints for Coulomb Satellite Formations," *AIAA/AAS Astrodynamics Specialists Conference*, No. 04-5213, 2004.

[15]Natarajan, A. and Schaub, H., "Hybrid Control of Orbit-Normal and Along-Track Two-Craft Coulomb Tethers," *AAS/AIAA Space Flight Mechanics Meeting*, No. 07-193, Jan.-Feb. 2007.

[16]Inampudi, R., *Two-Craft Coulomb Formation Study About Circular Orbits and Libration Points*, Ph.D. thesis, University of Colorado, 2010.

[17]Wang, S. and Schaub, H., "One-Dimensional 3-Craft Coulomb Structure Control," *7th International Conference on Dynamics and Control of Systems and Structures in Space*, June 2006, Greenwich, London, England.

[18]Jasch, P., Hogan, E., and Schaub, H., "Stability Analysis and Out-of-Plane Control of Collinear Spinning Three-Craft Coulomb Formations," *AAS/AIAA Spaceflight Mechanics Meeting*, No. 12-151, Jan.-Feb. 2012, Charleston, SC.

[19]Natarajan, A., *A Study of Dynamics and Stability of Two-Craft Coulomb Tether Formations*, Ph.D. thesis, Virginia Polytechnic Institute and State University, 2007.

[20]Jones, D. R., "Optimal Reconfiguration of Coulomb Formations Along Invariant Manifolds," *AAS/AIAA Spaceflight Mechanics Meeting*, No. 12-104, Jan.-Feb. 2012, Charleston, SC.

[21]Jones, D. R. and Schaub, H., "Optimal Reconfigurations of Two-Craft Coulomb Formations along Manifolds," Submitted for Publication to Acta Astronautica.

[22]Russell, R. and Lam, T., "Designing Ephemeris Capture Trajectories at Europa Using Unstable Periodic Orbits," *Journal of Guidance, Control, and Dynamics*, Vol. 30, No. 2, March-April 2007, pp. 482–491.

[23]Clohessy, W. and Wiltshire, R., "Terminal Guidance System for Satellite Rendevous," *Journal of the Aerospace Sciences*, Vol. 27, No. 9, 1960, pp. 653–658.

[24]Bittencourt, J., *Fundamentals of Plasma Physics*, Springer-Verlag New York, Inc,, 2004.

[25]Stiles, L., Seubert, C., and Schaub, H., "Effective Coulomb Force Modeling in a Space Environment," *AAS/AIAA Spaceflight Mechanics Meeeting*, No. 12-105, Jan.-Feb. 2012, Charleston, SC.

[26]Guckenheimer, J. and Holmes, P., *Nonlinear Oscillations, Dynamical Systems, and Bifurcations of Vector Fields*, Springer, New York, 1997.

[27]Natarajan, A. and Schaub, H., "Linear Dynamics and Stability Analysis of a Two-Craft Coulomb Tether Formation," *Journal of Guidance, Control, and Dynamics*, Vol. 29, No. 4, July-August 2006, pp. 831–838.

[28]Tsui, C.-C., *Robust Control System Design: Advanced State Space Techniques*, Marcel Dekker, New York, 2nd ed., 2004.

[29]Boley, D. and Lu, W.-S., "Measuring How Far a Controllable System is from an Uncontrollable One," *IEEE Transactions on Automatic Control*, Vol. 31, No. 3, 1986, pp. 249–251.